Implications of halide leaching on chlorine-36 studies at Yucca Mountain, Nevada

Guoping Lu, Eric L. Sonnenthal, and Gudmundur S. Bodvarsson

Earth Sciences Division

Lawrence Berkeley National Laboratory

Berkeley, CA 94720, USA

Abstract. Chlorine-36 was generated from nuclear tests in the 1950s and 1960s and has been used to identify fast flow paths at Yucca Mountain, the potential repository for high-level nuclear wastes (Fabryka-Martin et al., 1993; 1997; 1998). Because of dissolution of chloride from the matrix during leaching, the measure of bomb-pulse as $^{36}Cl/Cl$ ratio runs into difficulties. Possible consequences may include dilution of bomb-pulses for samples from strata with a high Cl concentration, dependencies of leaching time and sample size. This work provides a mathematical solution to leaching processes and examines the role of sample leaching in chlorine-36 studies at Yucca Mountain. A one-dimensional analytical model is developed for leaching of halide in composite media (rock matrix and water) to accommodate variable diffusivity. The concentration of leachate is obtained by taking into account the volumes of water and rock in different setups, including duration, chip sizes, and gravity settlement of the water-rock mixture. The model demonstrates that the chance of possible discovery of a $^{36}Cl/Cl$ bomb-pulse signal is severely diminished under longer leaching times and smaller fragment sizes. The bomb-pulses are likely

discovered within 5 hours, with leaching times less than 5 hours being more likely to exhibit a bomb-pulse signal.

Key words: chlorine-36, leaching, bomb-pulse, Yucca Mountain, fast flow-path

1. Introduction

Located within a semi-arid region in the western U.S., Yucca Mountain, Nevada, is a potential site for the U.S. Department of Energy high-level nuclear waste repository. The potential repository resides in an unsaturated zone (UZ) with a thickness of several hundred meters. Its area location is shown in Figure 1, along with the surface projection of the 8-km long Exploratory Studies Facility (ESF) tunnel, locations of boreholes, and traces of faults. Because the layers of strata are approximately parallel with the land surface, the ESF tunnel exposes the Tiva Canyon welded tuff (TCw) units and the Paintbrush nonwelded tuff (PTn) units at both north and south ramps, and the Topopah Spring welded tuff (TSw) in the main drift. The pore waters generally have higher Cl concentration in the TCw and PTn units and lower concentration in the TSw unit (Sonnenthal and Bodvarsson, 1999; Yang et al., 1998a,b; 1996).

Chlorine-36 has been used for dating groundwater and identifying fast flow paths (Bentley, 1986; Fabryka-Martin et al., 1993, 1997, 1998). Chlorine-36 can be naturally generated in the atmosphere, be carried in precipitation and subsequently enter the ground. Because of its long half-life of 308,000 years, chlorine-36 has been successfully used to date very old groundwater (Bentley, 1986). Another important application of chlorine-36 is to semi-quantify the movement of very young water (the focus of this

paper), taking advantage of chlorine-36 bomb-pulse input from nuclear tests from 1952 to 1958 (Fabryka-Martin et al., 1993, 1997, 1998). Whether it is naturally generated or created from the nuclear tests, chlorine-36 would have undergone a number of different processes, especially evapotranspiration, before it enters the ground from precipitate or run off. To account for the effect of these processes on ^{36}Cl, the chlorine-36 signatures are usually expressed as $^{36}Cl/Cl$ ratio (Bentley, 1986).

Because bomb-pulses are relatively young input, they are used to identify fast flow paths (faults or fractures) in relatively impermeable media (rock matrix). A recent study at Yucca Mountain indicates such fast flow paths along some fault zones or fractures in the unsaturated zones (UZ) (Fabryka-Martin et al., 1997; 1998). The finding has generated great interest from both the scientific community and the public. But interpreting the $^{36}Cl/Cl$ ratio as bomb-pulse signals may be problematic because the values of bomb-pulse signals may be skewed by Cl from sources other than the original ^{36}Cl (e.g., the chlorine leached from rock matrix and fluid inclusions).

Systematic deviation may result from the difference in the setup of chlorine leaching. The effect of Cl leaching from matrix was observed when samples pulverized by the ream bit in the borehole drilling were tend to have systematically lower $^{36}Cl/Cl$ ratio (Fabryka-Martin et al.1998; Liu et al., 1995). This finding indicates that the $^{36}Cl/Cl$ ratio may in fact be a function of the dissolution of the chloride from the rock matrix and whatever consequent dilution of chlorine-36 signature or bomb-pulse. The dilution is confirmed through review of the existing chlorine-36 data (from Fabryka-Martin et al., 1997) showing that the distribution of $^{36}Cl/Cl$ ratios have been scaled down with the increase of Cl concentration (Sonnenthal and Bodvarsson, 1999). Leaching of chlorine in

the matrix (existing prior to nuclear bomb-testing in early 1950s) in the sample preparation complicates the study of chlorine-36.

The results from Fabryka-Martin et al. (1997) showed that the bomb pulses are present not only in fault zones but also in fractured zones between faults, but were not found in somewhat expected locations (Wolfsberg et al, 2000; Fabryka-Martin et al., 1997). For example, the south ramp of the ESF is reasoned most likely to have bomb-pulse due to a thin overlying PTn; however, the measured data indicate virtually no-bomb pulse ^{36}Cl signals in this area (Fabryka-Martin et al., 1997).

To validate the bomb-pulse of chlorine-36 present at ESF, researchers from USGS collected tritium data at or near locations where samples have been collected for Cl-36 analysis (Patterson, 2000). Tritium has a half-life of 12.43 years. Estimate of tritium concentration is about 5–8 TU in precipitation near Yucca Mountain prior to the testing of nuclear weapons (Patterson, 2000). Therefore, water with tritium in excess of 1 TU must contain some component of water that infiltrated the site within the last 50 years.

Discrepancies are observed when these chlorine-36 bomb-pulse signals are compared with tritium data. While the Cl-36 data indicate the presence of post-bomb Cl-36 at numerous locations within the Drill Hole Wash and Sundance faults (Figures 1 and 2), that presence of tritium bomb-pulses appears to be isolated in the northern part of the ESF (Patterson, 2000). In addition, the Cl-36 data indicate that the South Ramp is devoid of any post-bomb water, whereas the tritium data indicate that post-bomb water is common within the South Ramp (Patterson, 2000).

This work is focused on the discussion of Cl dissolution in the leaching and its implication on chlorine-36 studies at Yucca Mountain. The results are expected to shed

some insights into the discrepancies of fast-flow path identifications. A leaching model is developed to simulate factors in leaching, including leaching time, size of rock chips, and whether the water rock mixtures are allowed to settle. Samples from different geological units are discussed with respect to rock properties such as porosity, saturation, and Cl concentration. Section 1 discusses chlorine-36 studies at Yucca Mountain. Section 2 is a conceptual model developed to explain the leaching processes. Section 3 provides an analytical model exploring the scenario of leaching of rock samples. Discussion of leaching time, size, and active leaching, as well as conclusions, are found in Sections 4 and 5.

2. Conceptual Leaching Models for ^{36}Cl Samples

Fabryka-Martin et al. (1997) collected rock samples from the field for chlorine-36 analysis by dry chipping or drilling. Usually a large rock sample collected from the field was hammered into rock chips for leaching. These rock chips most probably have fracture surfaces along which bomb pulses have percolated if fast path exists (Figure 3). Therefore, bomb-pulse ratios should be lying within in a thin layer of rock mass near the fracture surface.

To leach the halide Cl out of the samples for ^{36}Cl analysis, the rock chips are merged in the leaching water. When the experiment begins, mass moves by diffusion from rock matrix of high concentration to the bulk leaching water of low concentration until equilibrium is established. A one-dimensional diffusion model of chloride across the interface of rock and water into the leaching agent water is conceptualized in Figure 4. The figure shows an infinite rock interfacing with an infinite reservoir bulk water. In this

conceptual model, bomb-pulse ratios are configured near the interface and the non-bomb-pulse halides are found deeper in the matrix.

3. Mathematical Model

In this section, we will develop a mathematical model to treat diffusion in composite media with different properties of diffusion, i.e., from matrix into the water body. Based on the preceding conceptual model, a one-dimensional diffusion model is progressively developed into a model suitable for representing leaching. We begin our discussion with a diffusion process in an infinite column to illustrate advancement of a concentration front. In this case, the source is confined within an area (one-dimension), which is similar to laboratory leaching in that the halides are originally confined within the rock chips. We then extend the system to composite media (rock and water) to accommodate porosity, saturation, and tortuosity variations. Furthermore, we limit the system within a finite domain, i.e., the infinite extensions of the rock-water column are replaced by two boundaries, one for the point center of rock chip and the other for the middle point in the water space between rock chips. Finally, we show how to remove the two boundaries to suite for our leaching problem.

To aid in understanding the effect from sample sizes, we build a relationship between chip sizes and the water spaces in between. We will also show how the one-dimensional model is successfully assembled for modeling the leaching process.

3.1 A Diffusion Process of Concentration Front in an Infinite Column of Porous Media

We start with the discussion of diffusion in an infinite column with confined sources. Initially, the porous media is saturated by two miscible liquids at different tracer concentrations. Between x_1 and x_2, the concentration is C_1; in all other location it is C_2. In the model, only molecular diffusion is considered; adsorption is neglected. The diffusion property of the porous media is assumed to be homogeneous.

Following the similar procedure by Jost (1952), the complete solution of concentration $C(x, t)$ at given time t and distance x is given by

$$\begin{aligned}\varepsilon(x,t) &= \frac{C(x,t)-C_2}{C_1-C_2} = \frac{1}{2\sqrt{\pi D t}}\int_{x-x_1}^{x-x_2}\exp(\frac{-x^2}{4Dt})dx \\ &= \frac{1}{2\sqrt{\pi D t}}\{\int_0^{x-x_1}\exp(\frac{-x^2}{4Dt})dx - \int_0^{x-x_2}\exp(\frac{-x^2}{4Dt})dx\} \\ &= \frac{1}{2}\{erf(\frac{x-x_1}{2\sqrt{Dt}}) + erf(\frac{x_2-x}{2\sqrt{Dt}})\} \\ &= \frac{1}{2}\{erf(\frac{x-x_1}{2\sqrt{Dt}}) - erf(\frac{x-x_2}{2\sqrt{Dt}})\}\end{aligned} \tag{1}$$

where $\varepsilon(x, t)$ is the scaled concentration, $D = D_f \alpha T^*$ is the diffusivity (L^2/T), D_f is the diffusion coefficient (L^2/T), α is the porosity of the porous medium, T^* is tortuosity in the porous medium, and *erf*( ) is the error function. The porosity, α, is used to account for the effective area of diffusion (assuming unit across sectional area). This solution is reduced to that of Jost (1952) when $x_1 = -x_2$.

3.2 Diffusion Concentration Front at Physical Discontinuity.

The above generalized solution for confined source is then extended to solve the concentration front across the interface of rock matrix and bulk water, where a discontinuity in diffusion properties exists. According to Fick's second law for

conservation of mass, the partial differential equations governing the halide distributions in the matrix ($x < 0$) and in the water ($x \geq 0$) are:

$$\begin{aligned} \partial C / \partial t &= D_1 \, \partial^2 C / \partial x^2, \qquad x < 0 \\ \partial C / \partial t &= D_2 \, \partial^2 C / \partial x^2, \qquad x \geq 0 \end{aligned} \tag{2}$$

where D_1 and D_2 are the diffusivities in porous media and water, respectively.

Initial conditions are:

$$\begin{aligned} t \leq t_0, \quad -\infty < x < x_1, \qquad & C = C_2 \\ x_2 < x < +\infty, \qquad & C = C_2 \\ x_1 \leq x < x_2, \qquad & C = C_1 \end{aligned} \tag{3}$$

Boundary conditions are:

$$\begin{aligned} t > t_0, \qquad x = \pm\infty, \qquad & \partial C / \partial x = 0 \\ x = +\infty, \qquad & C = C_2 \\ x = -\infty, \qquad & C = C_2 \\ x = 0, \qquad & C\big|_{x \to 0^-} = C\big|_{x \to 0^+} \\ x = 0, \qquad & D_1 \partial C / \partial x\big|_{x \to 0^-} = D_2 \partial C / \partial x\big|_{x \to 0^+} \end{aligned} \tag{4}$$

Noting that the above partial differential equation is linear, we can solve the partial differential equation by assuming that the solution takes following form, with concentration in the region $x < 0$ given by:

$$\begin{aligned} \varepsilon_1(x) &= \frac{C(x) - C_2}{C_1 - C_2} \\ &= \frac{1}{2}\left\{\left[erf\left(\frac{x - x_1}{2\sqrt{D_1 t}}\right) - erf\left(\frac{x - x_2}{2\sqrt{D_1 t}}\right)\right] + A\left[erf\left(\frac{-x - x_1}{2\sqrt{D_1 t}}\right) - erf\left(\frac{-x - x_2}{2\sqrt{D_1 t}}\right)\right]\right\} \end{aligned} \tag{5}$$

For region x ≥ 0, we have:

$$\varepsilon_2(x) = \frac{C(x) - C_2}{C_1 - C_2} = c(x) \qquad (6)$$
$$= \frac{1}{2} B\{erf(\frac{x - x_1}{2\sqrt{D_2 t}}) - erf(\frac{x - x_2}{2\sqrt{D_2 t}})\}$$

where A and B are yet unknown constants. By inserting Eqs.5-6 into Eqs. 2-4, we obtain:

$$A = (E - N)/(E + N) \qquad (7)$$
$$B = 2/(E + N)$$

where E and N are given as

$$E = \frac{erf(x_2/(2\sqrt{D_2 t})) - erf(x_1/(2\sqrt{D_2 t}))}{erf(x_2/(2\sqrt{D_1 t})) - erf(x_1/(2\sqrt{D_1 t}))} \qquad (8)$$
$$N = \sqrt{D_2/D_1}\,\frac{\exp(-x_2^2/(4D_2 t)) - \exp(-x_1^2/(4D_2 t))}{\exp(-x_2^2/(4D_1 t)) - \exp(-x_1^2/(4D_1 t))}, \qquad x < 0$$

when $D_1 = D_2$, N=1, that is, when both the matrix and the bulk water have the same diffusion property, the solution reduces to the special case (Eq. 1) in Section 3.1.

In Eqs. 5 and 6, we use a lumped C in which porosity and saturation are factored into the measured pore water concentration C (i.e., pore water C multiplied by both porosity and saturation).

3.3 Diffusion of Confined Sources in Composite Media inside Finite Domain

We developed a mathematical model to simulate the diffusion from the matrix to the bulk water. The domain is limited from the center point of the matrix to the center point of the water spaces in between. This system can be viewed as a finite system. Consequently, the two center-points are the boundaries. If the column of water is of finite

length, r_l, the condition in which the concentration tends to zero as x approaches infinity is replaced by the condition in which no flux of diffusing halide occurs across through the center point of the water space between rock fragments. Similarly, when the column of matrix is of finite length, r_m, the condition in which the concentration tends to zero as x approaches infinity is replaced by the condition that no flux of diffusing halide across through the center point of the matrix. Thus, we have the following boundary conditions for the two boundaries:

$$\partial C / \partial x = 0, \quad x = r_l \ and \ x = r_m \tag{9}$$

We employ reflection and superposition methods for a solution that satisfies the boundary conditions. We have seen that this condition is satisfied if the concentration curve are considered to be reflected at the boundary and the reflected curves superposed on the original one. In the finite system we are now considering, there are two concentration fronts, one to the right of matrix and the other to the left of the matrix. The right curve reflected at x = r_l is reflected again at x = r_m, and again at x = r_l, and so on, with the result of each successive reflection superposed on the original curves (6). Similarly, the left curve reflected at x = r_m is reflected again at x = r_l and again at x = r_m, and so on, with the result of each successive reflection superposed on the original curves (Eq. 5). Throughout superposition of the reflected curves, the concentration fronts across the interface are required to satisfy boundary conditions at $x = 0$.

3.4 One-Dimensional Leaching Model

Rock chips can be distinguished as two end-members, that is, chips with bomb-pulse and chips without any bomb-pulse. These two end-members give different inputs to the leachate. In this subsection, we show how an individual chip and its surrounding water body are represented by a one-dimensional model to simulate the leaching process. For the convenience of derivation, rock mass and chips are converted into spheres with uniform weight. From this we will find out how many spheres have bomb-pulse ratios of Chlorine-36. Then we derive the bulk concentration of leachate from water in contact with these two types of spheres.

The number (n_r) of spheres broken from a rock mass of M grams can be represented as

$$n_r = \frac{M}{\pi / 6 R_m^3 d_r} \tag{10}$$

where R_m is the diameter of the rock chips and d_r is rock density (assumed to be 2.56 g/cm^3 for this work). Total surface area S for these (n_r) number of chips become

$$S = n_r \pi R_m^2 \tag{11}$$

And the surface area with bomb-pulse is calculated as

$$S_p = n_f \pi R_0^2 / 4 = (\pi / 4) n_f [6M /(\pi d_r)]^{2/3} \tag{12}$$

where n_f is the number of fractures dissecting the original mass (through the center point). R_0 is the diameter of the sphere with the same volume as the original rock. Because of the difficulty in determining how many fractures inside a particular rock mass have bomb-

pulse, we assumed that the original rock mass was dissected by a certain number of fractures and further assumed that the fractures run through the center of the rock mass.

Therefore the number of spheres with bomb-pulse ratios (with equivalent surface area S_p) can be calculated with the following formula,

$$n_p = \frac{S_p}{\pi R_m^2} = \frac{n_f \pi R_0^2 / 4}{\pi R_m^2} = \frac{n_f}{4R_m^2}[6M/(\pi d_r)]^{2/3} \tag{13}$$

where n_p is the number of spheres with bomb-pulse ratios. The bulk concentration of leachate can be found by considering the amount of water in contact with chips of these two types.

Through the proceeding derivation, the numbers of chips with and without bomb-pulse ratios are known for Cl distribution of end-members. With this information, we are able to find the amount of trapped water in contact with bomb-pulse chips and the amount in contact with chips without bomb-pulse.

Then overall concentration of the leachate can be calculated through,

$$C = \frac{C_l V_{trw} + C_{fw} V_{fw}}{V_{trw} + V_{fw}} \tag{14}$$

where C_l is composite concentration of trapped water, C_{fw} is the concentration in the free water over the chips, V_{trw} is the volume of trapped water between chips, and V_{fw} is the volume of free water over the chips. The calculation of C_l through the leaching model is discussed later.

The relationship of rock chips and water spaces between them varies from one experiment to another. For demonstration purpose, we have the following formula, by assuming the rock spheres are stacked as cubes,

$$r_l = (\sqrt{2} - 1) R_m / 2 \tag{15}$$

where r_l is the distance from the sphere surface to the middle of the water space between them. The water trapped between is the spheres is calculated using the following formula:

$$V_{trw} = n_r \ (R_m^3 - \frac{1}{6}\pi \ R_m^3) \tag{16}$$

By assuming the total water weighs the same as that of rock chips, the free water on the top of the rock spheres is

$$V_{fw} = V_w - V_{trw} = M / d_w - n_r \ (R_m^3 - \frac{\pi}{6} R_m^3) \tag{17}$$

where d_w is the density of the water (assumed 1.0 gram/Liter in our model).

To derive the composite concentration C_l in trapped water between chips, we need to determine (among all the trapped water) how much water is in contact with bomb-pulse chips and not. The water in contact with the surface containing bomb-pulses will receive bomb-pulse components and matrix components, while the water in contact with chips not containing bomb-pulses will leach matrix component directly. Therefore, the water in contact with chip spheres with or without bomb-pulse are calculated by:

$$V_p = n_p(R_m^3 - \frac{\pi}{6}R_m^3) \tag{18}$$

$$V_{np} = V_{trw} - V_p = (n_r - n_p)(R_m^3 - \frac{\pi}{6}R_m^3)$$

where V_p and V_{np} representing volumes of water in contact with spheres with or without bomb-pulse, respectively.

Finally, the composite concentration in trapped water space is related to bomb-pulse surface by

$$C_l = \frac{C_p V_p + C_{np} V_{np}}{V_p + V_{np}} \tag{19}$$

where C_p and C_{np} are the concentration from chips with and without bomb-pulse. This C_l is used in Eq. 14 to derive the leachate concentration.

4. Discussion

We use our model to demonstrate the leaching of halide (Cl) and its effect on the ^{36}Cl/Cl ratio. We distinguish rock chips with and without bomb-pulse ratios and assign them as two end-members.

Basic assumptions need to be expressed for our model. The soaking of rock chips at onset of the leaching is finished in very short time and does not affect the outcome of the leaching. The rock mass is 1,000 grams, and leaching water has the same weight as the rock mass, thus rock chips were completely merged under the water. Rock chips are

assumed to have uniform size. The bomb pulse is distributed within a thin 1 mm layer from the fracture surface and assumed to have $^{36}Cl/Cl$ of 150,000, which is about at the low value between two peaks (Fabryka-Martin et al, 1997). This peak is assumed to have been carried by rainwater which has an average Cl concentration of 0.55 mg/L (data from Fabryka-Martin et al, 1997). The number of idealized straight fractures dissecting the rock samples and having bomb-pulses are equivalent to be a total of 2. It is arbitrary and used to show a sample carrying sufficient bomb-pulse to make the model meaningful.

Inputs to the leaching model include information about Cl concentration, porosity and saturation for strata units TCw, PTn, and TSw at Yucca Mountain (Tables 1, 2). As will be discussed later, porosity and concentration play very important roles in the leaching and thus the recovery of bomb-pulse ratio signals. Even though fluid inclusions possibly provide chloride into the leachate, they are not included in our model because no relevant data are available. In our calculation, tortuosity was assigned the same values as porosity (Moridis and Hu, 2000; Farrell and Reinhard, 1994; Grathwohl, 1998). Porosity and saturation in the matrix are used in the concentration term to get the actual gradient after the rock chips have been soaked.

In the following discussion, we evaluate the leaching setup, including leaching time, chip sizes and effect from whether the leaching is gravity-settled. Leachate concentration versus time is plotted in Figure 6. Active or passive leaching is demonstrated in Figure 7, with the effect of sizes in leaching shown in Figure 8.

4.1 Time Dependence of the Leaching Process

Leaching is strongly dependent on time. The peak $^{36}Cl/Cl$ ratio generally occurs within 2 hours of leaching, and the bomb-pulse signal can be discovered at most within first 5 hours of leaching (Figure 6).

Bomb-pulse ratios are more strongly suppressed in samples from TCw and PTn than in TSw. This is explained by the "masking" effect produced by the high concentration of Cl in TCw and PTn units (Sonnenthal and Bodvarsson, 1999). This effect demonstrates why almost no bomb-pulses are found in the North Ramp, and no bomb-pulse at all is found in the South Ramp (Figure 2). Judging by the Cl concentration alone, the bomb-pulse signals from TCw should have been more suppressed than those from PTn, but in fact they are actually almost identical. This is because the effect of higher concentration of TCw sample is offset by its lower diffusivity, which results primarily from the lower porosity (Table 1).

For samples from the TSw unit, the leaching of bomb-pulse ^{36}Cl reaches its peak very fast because of both very low porosity and low Cl concentration. For the same reason, the bomb-pulse signals are less suppressed. This explains why many bomb-pulse signals are observed in the main drift.

According to the leaching curve for samples from TSw, ^{36}Cl reaches a plateau early and remains at that level. Because of low Cl concentration, and very low porosity of TSw, samples result in slow leaching from matrix. Thus the Cl concentration of leachate is always low (Figure 6b).

To build the confidence of using ^{36}Cl as bomb-pulse signal, more work is desired to investigate effect from variations in key parameters such as concentration and porosity. A

stochastic analysis or Monte Carlo is an appropriate approach. The model must be calibrated with laboratory data.

4.2 Active or Passive Leaching Process

Active leaching requires that the rock water mixtures be disturbed or at least tumbled one or twice during leaching. Passive leaching means no disturbance of the samples. During sample tumbling, the leachate concentration was homogenized. The previously established leaching profile is replaced with a new, sharp concentration front. To approximate the tumbling effect, the relevant terms for concentration in water C_2 in Eq. (6) were substituted with the new homogenized concentration.

Because samples were not disturbed constantly during leaching (Fabryka-Martin et al., 1997), only one tumbling was simulated. Figure 7 shows the effect of one tumbling on Cl in the middle of the 48-hour leaching for TCw samples. The importance of occasional tumbling of the samples is relatively small compared to time and size factors, in term of bomb pulse ratio, but is dramatic in leaching of Cl and ^{36}Cl (Figure 7).

4.3 Size Dependence of the Leaching Process

The size of rock-chips affects the bomb-pulses differently, depending on the sampling locations (Figure 8). The most significant affected is the TSw samples. Bomb-pulse ratios are more difficult to produce when leaching with smaller sizes of rock chips. Combined with the time effect discussed above, samples with smaller sizes are rarely found even to have bomb-pulse. (This is true even for main drift samples, all in TSw). Thus, we believe that the key to the chlorine-36 study lies in these two factors, leaching time and sample

sizes. The size effect on samples from the TCw and the PTn is small, considering their high Cl concentration and relatively high porosity (Figure 8).

5. Conclusions

This paper tries to address some issues of chlorine-36 studies in the UZ at Yucca Mountain. The application of chlorine-36 to semi-quantify fast flow paths (less than 50 years) runs into trouble because of the dissolution of halide (Cl) from the matrix during leaching. Because Cl is directly related to the ^{36}Cl studies as the bomb-pulse signals ^{36}Cl/Cl, the distribution of Cl in the Yucca Mountain is of great interest.

Review of the existing chlorine-36 data (Fabryka-Martin et al., 1997) finds that the ^{36}Cl/Cl ratios decrease with increasing Cl concentration (Sonnenthal and Bodvarsson, 1999). To understand this dilution problem with respect to the ^{36}Cl/Cl ratio, we developed a leaching model to simulate the effects from the variations in the leaching process, including time, sizes of rock chips, and the gravity settlement of the rock-water mixtures (passive or active leaching).

Model results show that the leachate concentration increases with time, and that the bomb-pulse can be mostly recovered within 5 hours into the leaching. Also, bomb-pulse ratios are sensitive to the sizes of rock chips and influenced by the difference between passive and active leaching.

Model results indicate that bomb-pulses are “masked” in the TCw and PTn when using the ^{36}Cl/Cl ratio to measure the signal, because of high Cl concentration and relatively high porosity. This corroborates the ‘masked’ effect observed by Sonnenthal and Bodvarsson (1999).

Acknowledgments

The authors would like to thank Andrew Wolfsberg for his useful discussions about ^{36}Cl studies at Yucca Mountain, Jennifer Hinds for the coordinate data of boreholes and ESF samples, Keni Zhang for his internal review comment, and Daniel Hawkes for his editorial work on the manuscript.

Reference

Bear, J., *Dynamics of Fluids in Porous Media*, Dover Publications, Inc., New York, New York, 1972.

Bentley, H. W., S. N. Davis, D. Elmore, and G. B. Swanick, Chlorine-36 dating of very old groundwater 2: Milk River aquifer, Canada, *Water Resourc. Res*., 22, 2003-2016, 1986.

Fabryka-Martin, J. T., H. R. Turin, D. Brenner, P. R. Dixon, B. Liu, J. Musgrave, and A. V. Wolfsberg, Summary Report of Chlorine-36 Studies as of August 1996. Milestone 3782M, LA-13458-MS, Los Alamos National Laboratory: Los Alamos NM, 1998.

Fabryka-Martin, J. T., A. V. Wolfsberg, P. R. Dixon, S. S. Levy, B. Liu, and H. R. Turin, Summary Report of Chlorine-36 Studies: Sampling, Analysis, and Simulation of Chlorine-36 in the Exploratory Studies Facility, Milestone 3783M, LA-13352-MS. Los Alamos National Laboratory: Los Alamos NM, 1997.

Fabryka-Martin, J. T., S.J. Wightman, W.J. Murphy, M.P. Wickham, M.W. Caffee, G.J. Nimz, J.R., Southon, P. Sharma, Distribution of chlorine-36 in the unsaturated zone at Yucca Mountain: An indicator of fast transport paths. Proc., FOCUS '93: Site characterization and model validation, held 26-29 September 1993, Las Vegas, NV (American Nuclear Society: La Grange Park, Illinois), pp. 58-68, 1993.

Farrell, J., and M. Reinhard, Desorption of halogenated organics from model solids, sediments, and soil under unsaturated conditions. 2. Kinetics. *Environmental Science and Technology*, 28(1), 63-72, 1994.

Grathwohl, P., *Diffusion in natural porous media: contaminant transport, sorption/desorption and dissolution kinetics*, Kluwer Academic Publishers, Boston, 1998.

Jost, W., *Diffusion in Solids, Liquids,* Gasses, Academic Press, New York, 1952.

Lide D. R., *CRC Handbook of Chemistry and Physics*, 82nd Edition, CPC Press LLC, Boca Raton, Florida, 2001.

Liu, B., J. T. Fabryka-Marin, A. V. Wolfsberg, B. A. Robinson, and P. Sharma, Significance of apparent discrepancies in water ages derived from atmospheric radionuclides at Yucca Mountain, Nevada. In *Water Resources at Risk*, W. R. Hotchkiss, J. S. Downey, E. D. Gutentag, and J. E. Moor, eds., pp. NH-52-NH-62. Minneapolis, Minnesota: American Institute of Hydrology, 1995.

Moridis, G., and Q. Hu, Radionuclide transport model under ambient conditions, Lawrence Berkeley National Laboratory, MDL-NBS-HS-000008 REV00, 2000.

Patterson, G. L., Low-level measurements of tritium in the unsaturated zone from the Exploratory Studies Facility beneath Yucca Mountain, Nevada, Geological Society of America Annual Meeting, Reno, Nevada, A-479-480, 2000, November 9-18, 2000.

Robinson, B. A., A. V. Wolfsberg, C. W. Cable, and G. A. Zyvoloski, An unsaturated-zone flow and transport model of Yucca Mountain, Los Alamos National Laboratory YMP milestone report 3468, October 1995.

Sonnenthal, E. L., and Bodvarsson, G. S., Constraint on the hydrology of the unsaturated zone at Yucca Mountain, NV from three-dimensional model of chloride and strontium geochemistry, *Journal of Contaminant Hydrology,* 38, 107-156, 1999.

Wolfsberg, A. V., K. Cambell, J. T. Fabryka-Martin, 2000. Use of chlorine-36 data to evaluate fracture flow and transport models at Yucca Mountain, Nevada. Dynamics of fluids in fractured rock, Geophysical Monograph 122, American Geophysical Union, Washington, D.C.

Wu, Y. S., J. Liu, T. Xu, C. Haukwa, W. Zhang, H. H. Liu, and C. F. Ahlers, UZ flow models and submodels, Lawrence Berkeley National Laboratory, MDL-NBS-HS-000006 REV00, 2000.

Yang, I. C., G. W. Rattray, and K. M. Scofield, Carbon and hydrogen compositions for pore water extracted from cores at Yucca Mountain, Nevada, Proceedings of the 8th International High-Level Radioactive Waste Management Conference, p.27-32, ACC: MOL. 1998-330.0135, American Nuclear Society, La Grange Park, Ill., 1998a.

Yang, I. C., P. Yu, G. W. Rattray, and D. C. Thorstenson, Hydrochemical investigations and geochemical modeling in characterizing the unsaturated zone at Yucca Mountain,

Nevada. U.S. Geological Survey Water Resources Investigation Report 98-4132, U.S. Geological Survey, Denver, Co., 1998b.

Yang, I. C., G. W. Rattray, and P. Yu, Interpretation of chemical and isotopic data from boreholes in the unsaturated-zone at Yucca Mountain, Nevada. Water Resources Investigation Report 96-4058. U.S. Geological Survey, Denver, Co., 1996.

Tables

Table 1. Diffusion parameters used in the leaching models*

Strata Unit	**porosity (%)†**	**saturation‡**	**tortuosity††**
TCw	17.0	0.775	0.170
PTn	34.5	0.425	0.345
TSw	9.5	0.875	0.095

*Diffusion coefficient for Cl in the water 2.032e-5 cm^2/s (Lide, 2001). †data from Wu et al. (2000); ‡data from Robinson et al. (1995); ††Tortuosity is approximated using porosity data.

Table 2. Chlorine concentrations (mg/L) and $^{36}Cl/Cl$ ($x10^{-15}$) used in the leaching model

Stratum Unit	**matrix**		**pulse**	
	Cl	$^{36}Cl/Cl$	Cl	$^{36}Cl/Cl$**
TCw	(50~170)* 110	600	(0.23~3.21) 0.55	150,000
PTn	(30~100) 65	600	(0.23~3.21) 0.55	150,000
TSw	30	600	(0.23~3.21) 0.55	150,000

* Number inside parenthesis indicates range.

** Peak in the bomb-pulse signal is estimated occurred in 1957 with a $^{36}Cl/Cl$ ratio of $217{,}000x10^{-15}$ (Fabryka-Martin et al., 1997).

Figure Caption

Figure 1. Area map of Yucca Mountain region showing the positions of the Exploratory Studies Facility (ESF) tunnel and selected boreholes. Other lines are fault lines: F1 Salitario Canyon fault, F2 Drill Hole Wash fault, F3 Sundance fault, F4 Ghost Dance fault, F5 Bow Ridge fault. Filled circles and thickened lines along the ESF are the USGS's sampling locations of tritium analyses.

Figure 2. Chlorine-36 signatures for both $^{36}Cl/Cl$ (delta) and ^{36}Cl (diamond) along the ESF tunnel (Data from Fabryka-Martin et al., 1997; 1998).

Figure 3. Schematic illustration of a rock sample with a single fracture.

Figure 4. Ideal diffusive transport from infinite rock to bulk leaching water. When the experiment begins, mass moves from rock matrix of high concentrations to the bulk leaching water of low concentrations: (a) infinite rock water column; and (b) diffusive process illustration.

Figure 5. Illustration of leaching processes with water rock mixture in a beaker.

Figure 6. Time-dependent leaching curves for samples from TCw, PTn and TSw units: (a) $^{36}Cl/Cl$, ^{36}Cl; and (b) Cl.

Figure 7. Effect of active leaching (one tumbling) at half way through the leaching for samples from TCw, PTn and TSw units: (a) $^{36}Cl/Cl$, ^{36}Cl; and (b) Cl.

Figure 8. Size dependence of leaching for rock samples from TCw, PTn, and TSw: (a) $^{36}Cl/Cl$; and (b) Cl.

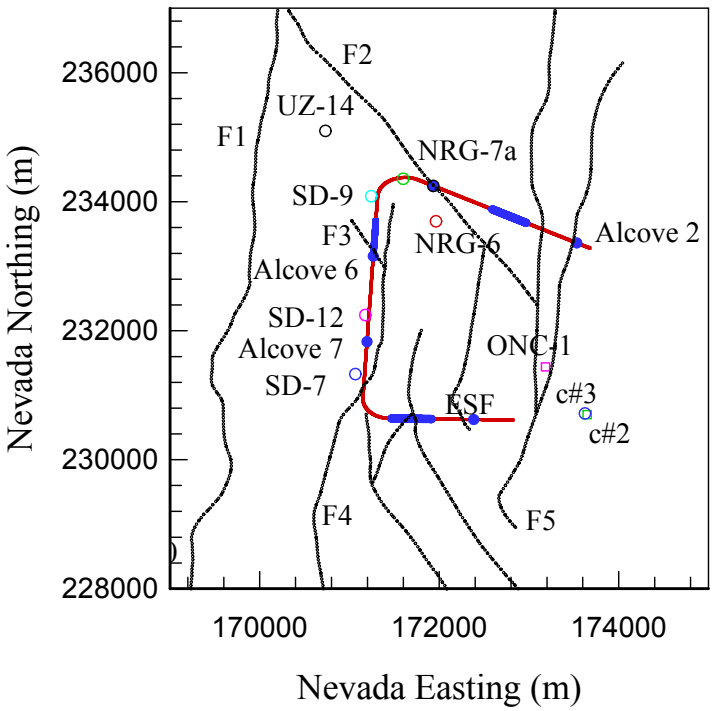

Figure 1. Area map of Yucca Mountain showing the position of the Exploratory Studies Facility (ESF) tunnel and selected boreholes. Other lines are fault lines: F1 Solitario Canyon fault, F2 Drill Hole Wash fault, F3 Sundance fault, F4 Ghost Dance fault, and F5 Bow Ridge fault. Filled circles and thick lines along ESF are the USGS's sampling locations of tritium analyses.

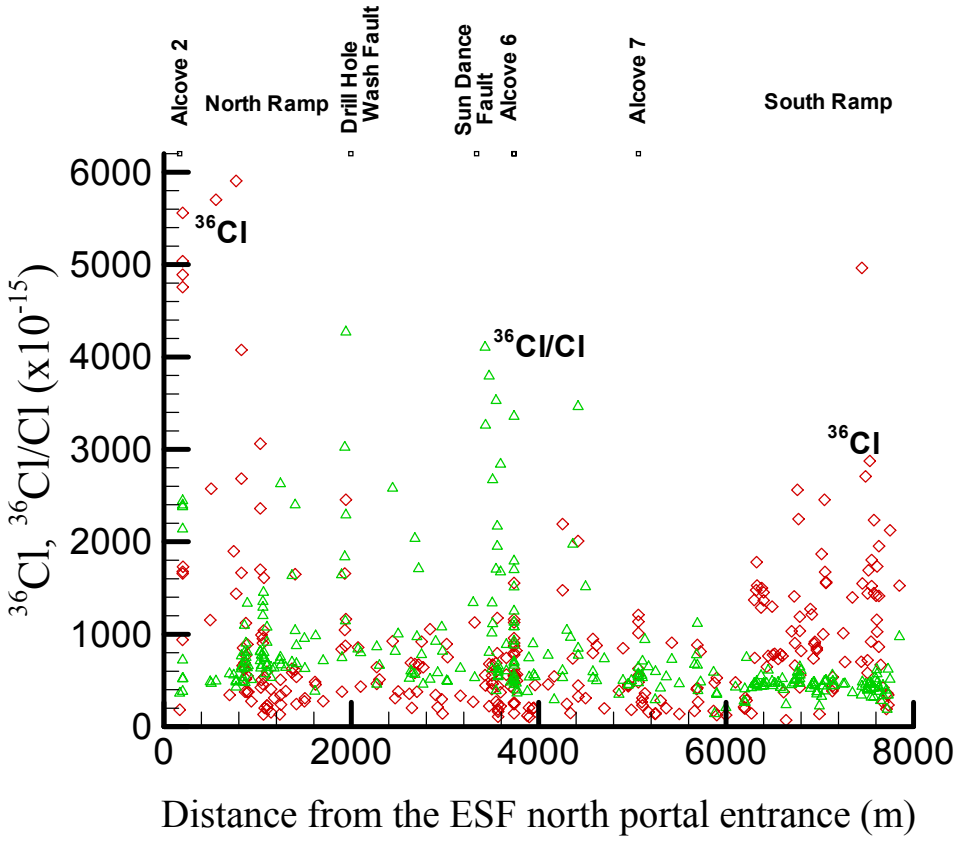

Figure 2. Chlorine-36 bomb-pulse signals as ^{36}Cl/Cl (delta) and ^{36}Cl (diamond) along the ESF tunnel (Data from Fabryka-Martin et al., 1997; 1998).

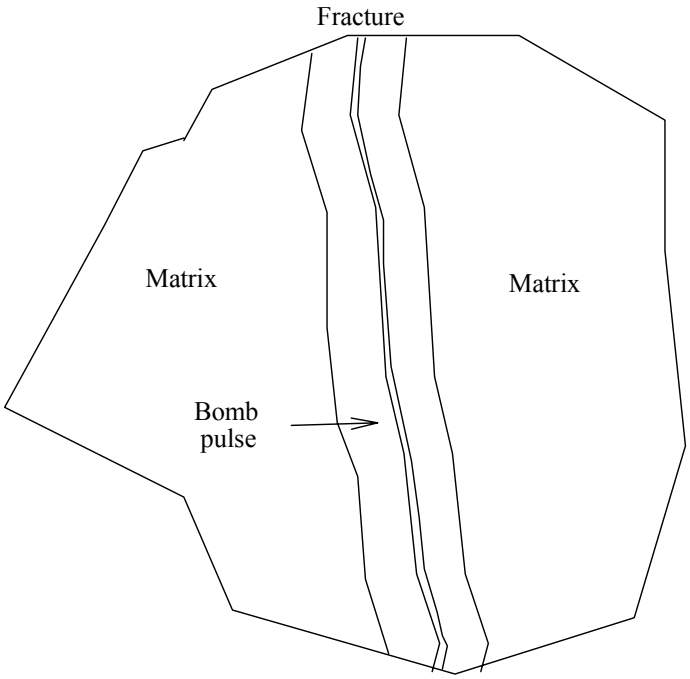

Figure 3. Schematic illustration of a rock sample with a single fracture

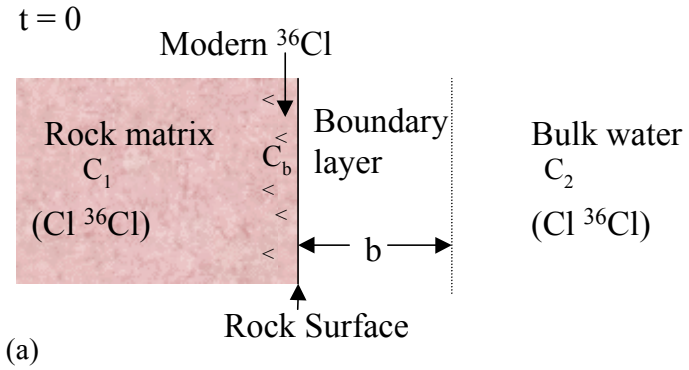

(a)

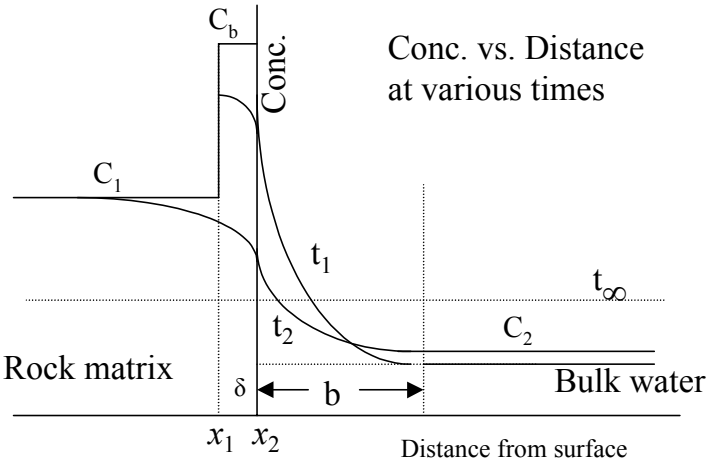

(b)

Figure 4. Ideal diffusive transport from infinite rock to bulk leaching water. When the experiment begins, mass moves from rock matrix of high concentrations to the bulk leaching water of low concentrations: (a) infinite rock water column; and (b) diffusive process illustration.

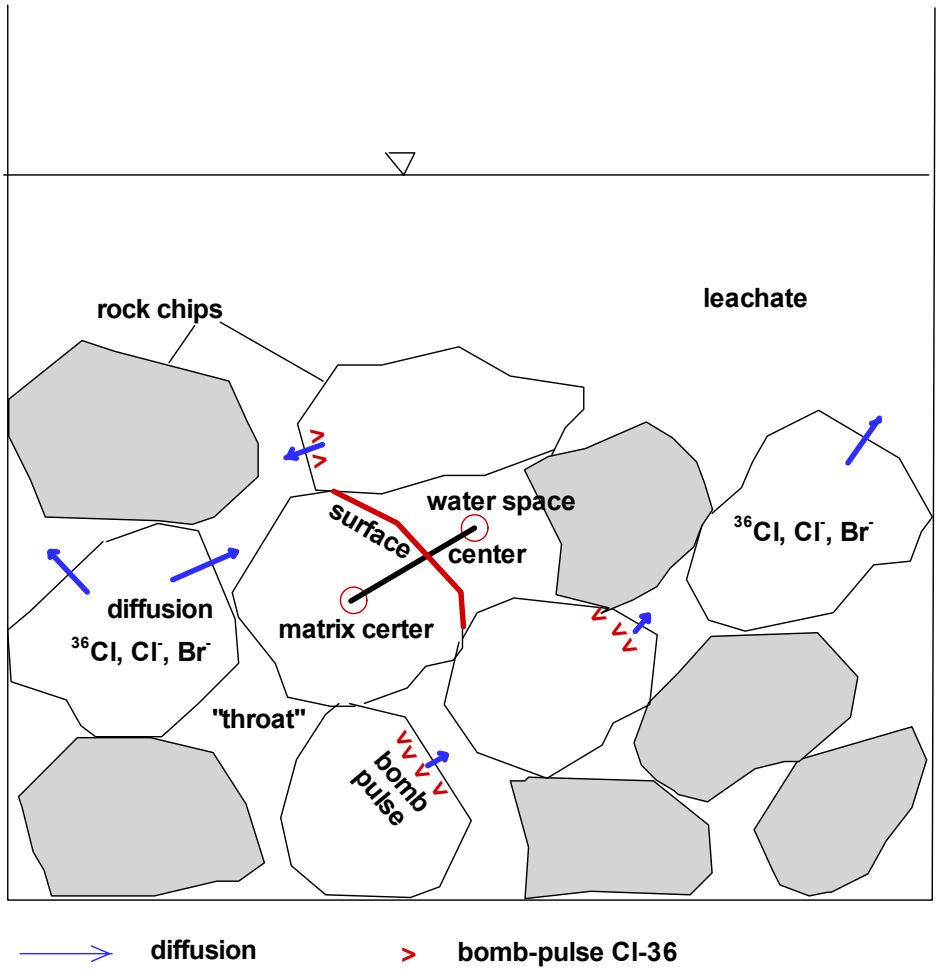

Figure 5. Illustration of leaching process with water rock mixture in a beaker.

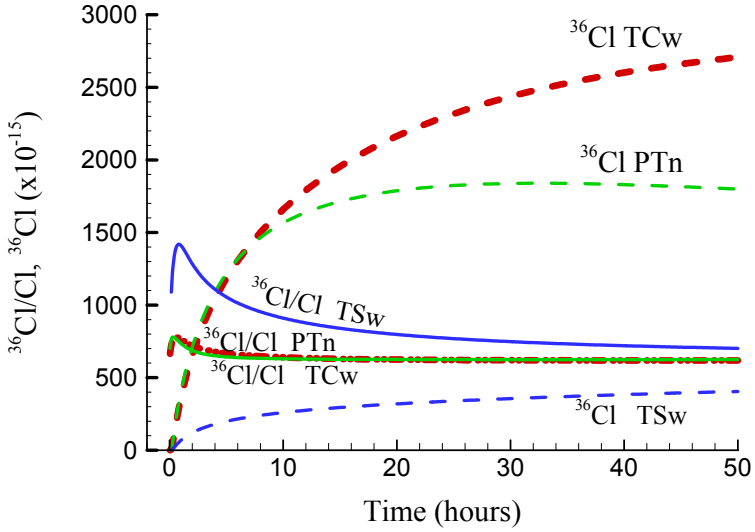

(a)

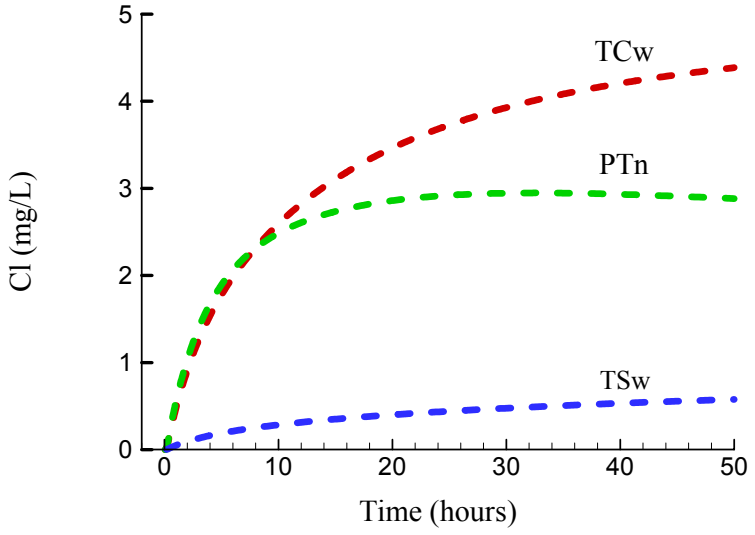

(b)

Figure 6. Time-dependent leaching curves for samples from Tcw, PTn, and TSw: (a) ^{36}Cl/Cl, ^{36}Cl; and (b) Cl.

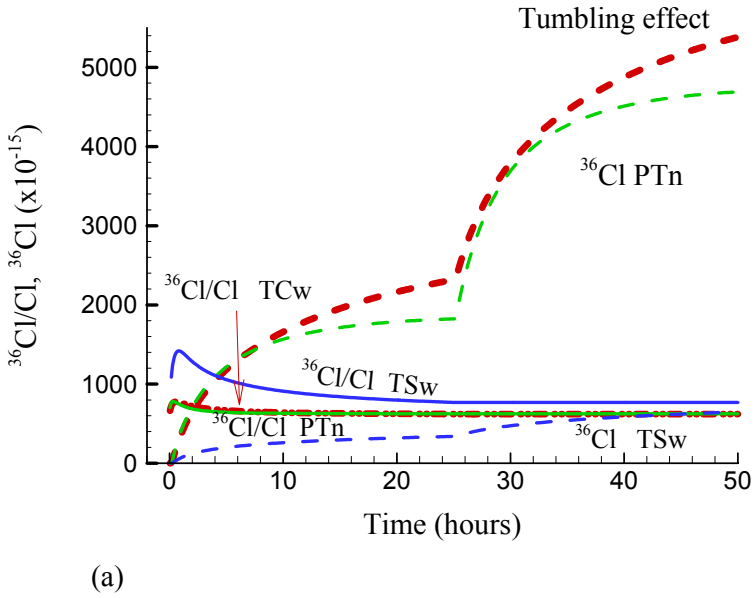

(a)

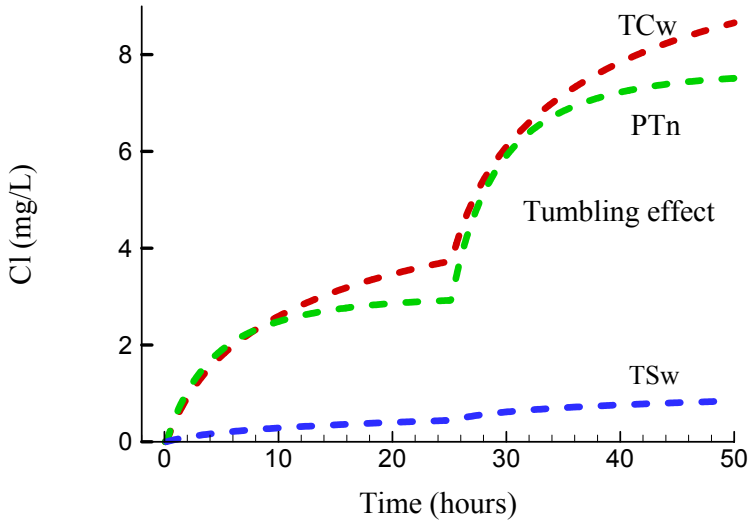

(b)

Figure 7. Effect of active leaching (one tumbling)at half way through the leaching of samples from TCw, PTn and TSw: (a) ^{36}Cl/Cl, ^{36}Cl: and (b) Cl.

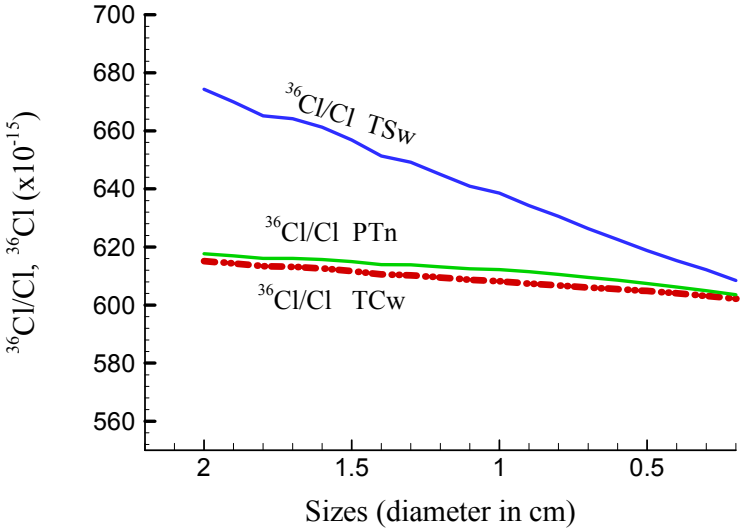

(a)

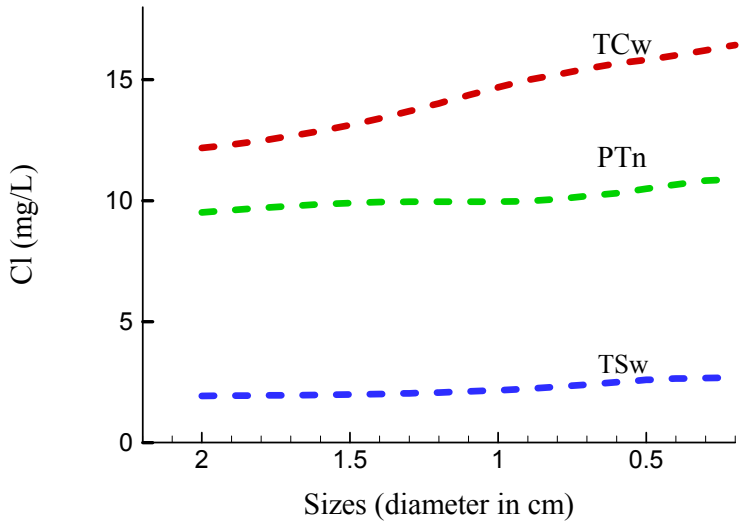

(b)

Figure 8. Size dependence of leaching for rock samples from Tcw, PTn and TSw: (a) ^{36}Cl/Cl; and (b) Cl.